Regional Correlation Among Ganglion Cell Complex, Nerve Fiber Layer, and Visual Field Loss in Glaucoma

Phuc V. Le,[1] Ou Tan,[2] Vikas Chopra,[1] Brian A. Francis,[1] Omar Ragab,[3] Rohit Varma,[4] and David Huang[2]

[1]Doheny Eye Institute and Department of Ophthalmology, Keck School of Medicine, University of Southern California, Los Angeles, California
[2]Casey Eye Institute, Oregon Health and Science University, Portland, Oregon
[3]Keck School of Medicine, University of Southern California, Los Angeles, California
[4]Illinois Eye & Ear Infirmary, University of Illinois-Chicago, Chicago, Illinois

Correspondence: David Huang, Casey Eye Institute, Oregon Health and Science University, 3375 SW Terwilliger Boulevard, Portland, OR 97239–4197; davidhuang@alum.mit.edu.

Submitted: November 27, 2012
Accepted: May 15, 2013

Citation: Le PV, Tan O, Chopra V, et al. Regional correlation among ganglion cell complex, nerve fiber layer, and visual field loss in glaucoma. *Invest Ophthalmol Vis Sci*. 2013;54:4287–4295. DOI:10.1167/iovs.12–11388

Purpose. To analyze the relationship among macular ganglion cell complex (GCC) thickness, peripapillary nerve fiber layer (NFL) thickness, and visual field (VF) defects in patients with glaucoma.

Methods. A Fourier-domain optical coherence tomography (FD-OCT) system was used to map the macula and peripapillary regions of the retina in 56 eyes of 38 patients with perimetric glaucoma. The macular GCC and peripapillary NFL thicknesses were mapped and standard automated perimetry (SAP) was performed. Loss of GCC and NFL were correlated with the VF map on both a point-by-point and regional basis.

Results. Correlation between GCC thickness and peripapillary NFL thickness produced a detailed correspondence map that demonstrates the arcuate course of the NFL in the macula. Corresponding regions within the GCC, NFL, and VF maps demonstrate significant correlation, once parafoveal retinal ganglion cell (RGC) displacement is taken into account.

Conclusions. There are significant point-specific and regional correlations between GCC loss, NFL loss, and deficits on SAP. Using these different data sources together may improve our understanding of glaucomatous damage and aid in the management of patients with glaucoma.

Keywords: optical coherence tomography, visual field, retinal nerve fiber layer, ganglion cell complex

Glaucoma is a spectrum of diseases characterized by optic neuropathy with loss of retinal ganglion cells. This results in characteristic changes to the optic nerve and corresponding visual field (VF) defects on standard automated perimetry (SAP). Vision loss in glaucoma is usually irreversible and progressive, thus early diagnosis and treatment are important in maintaining visual function and preventing vision loss. However, diagnosis of early glaucoma can be difficult. Because structural damage may be detectable prior to loss on SAP,[1] several technologies aimed at providing objective and quantitative measurements of the retina have been used to attempt to improve diagnostic accuracy and reproducibility. These include optical coherence tomography (OCT), scanning laser topography, and scanning laser polarimetry. Their uses in the diagnosis and management of patients with glaucoma have recently been reviewed.[2–4]

With the development of Fourier-domain OCT (FD-OCT), it is now possible to map retinal substructures over a wide area. One of these parameters is the ganglion cell complex (GCC). It is composed of the nerve fiber layer (NFL), the ganglion cell layer, and the inner plexiform layer, corresponding to the axons, cell bodies, and dendrites of the retinal ganglion cells. Given the importance of the macula in visual function, several recent studies, including our own, have focused on GCC parameters within the macula.[5–14] A similar parameter, which excludes the retinal NFL, termed ganglion cell layer plus inner plexiform layer (called GCL+ or RGC+), has also been recently studied in the context of glaucoma.[15–20] Studies of macular GCC and GCL+ have shown that they have similar diagnostic power to peripapillary NFL parameters. Moreover, glaucomatous damage to the macula can occur early in the disease and may be missed or underestimated by standard 24-2 VF test, which only sparsely samples macular vision.[20]

Our aim is to help clinicians interpret maps of GCC loss together with NFL and VF maps in the management of glaucoma patients. To help establish the boundaries between corresponding zones of the GCC, NFL, and VF maps, we generated detailed point-by-point correlation maps. We then divided the GCC map into four zones and established correlation with corresponding NFL and VF regions.

Methods

Study Population

Subjects in the perimetric glaucoma (PG) group and the normal (N) group of the longitudinal Advanced Imaging for Glaucoma Study (provided in the public domain at www.AIGStudy.net) from the University of Southern California (USC) and University of Pittsburgh Medical Center (UPMC) sites between the periods

Investigative Ophthalmology & Visual Science

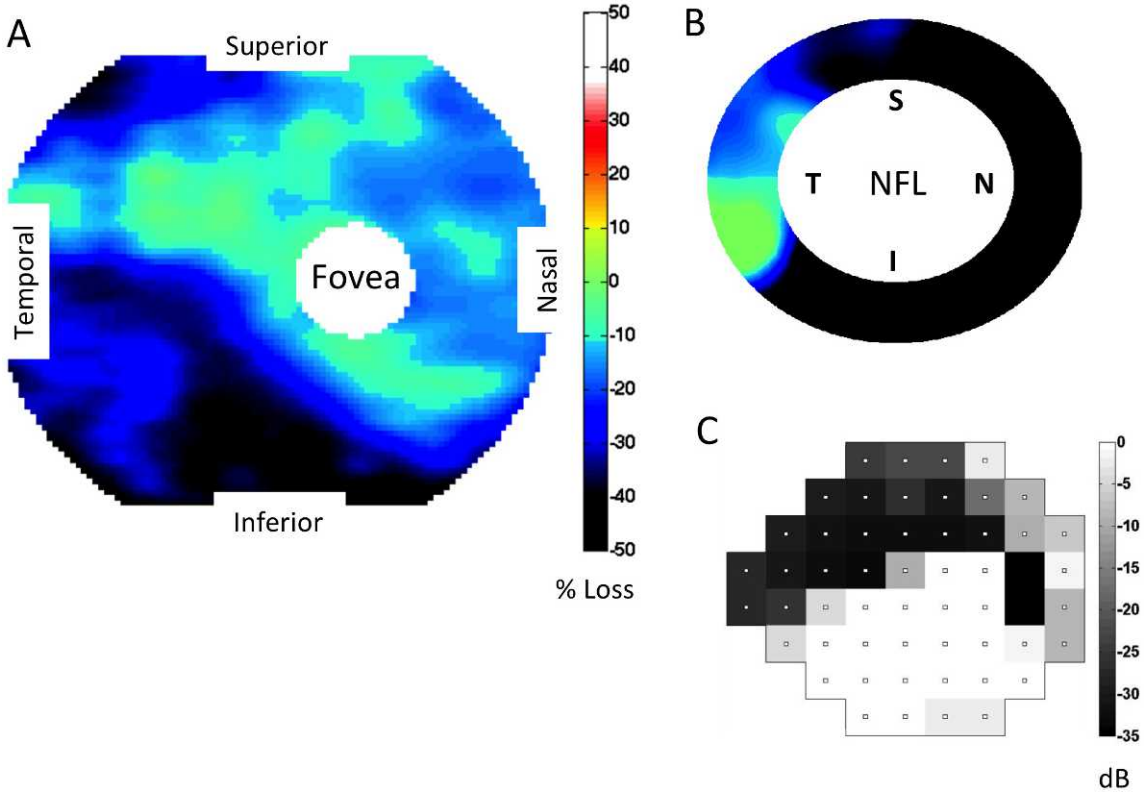

Figure 1. GCC, NFL, and VF maps in an eye with predominantly superior field defect. (**A**) Macular GCC thickness map, expressed as percent loss. (**B**) Peripapillary NFL thickness map, also expressed as percent loss. Same color scale as in (**A**). (**C**) The Humphrey 24-2 VF TD, displayed graphically. This eye has a large area of inferior ganglion cell complex (GCC) thinning encroaching on the fovea. There is corresponding peripapillary NFL loss inferiorly and a dense superior arcuate defect affecting fixation. NFL, nerve fiber layer; VF, visual field.

of 2003 and 2007 were included. The complete study criteria are available on the Web site. Briefly, the PG subjects had characteristic glaucomatous VF loss and optic nerve head (ONH) changes. Glaucomatous VF loss was defined as corrected pattern standard deviation ($P < 0.05$), or glaucoma hemifield test ($P < 1\%$) on Humphrey Swedish interactive thresholding algorithm (SITA) standard 24-2 visual field. ONH changes included thinning, notching, optic nerve hemorrhage, or cup/disc asymmetry of more than 0.2.

The criteria for normal were defined previously,[5] but can briefly be described as having IOP less than 21, normal Humphrey SITA 24-2, central corneal thickness greater than 500 μM, a normal-appearing ONH, a normal-appearing NFL, an open anterior chamber angle, and no history of chronic ocular or systemic steroid use. Eyes that were classified as ocular hypertensive, glaucoma suspect, or pre-perimetric glaucoma were not included in this study.

Written, informed consent was obtained from all participants. Procedures followed the tenets of the Declaration of Helsinki and the protocol was approved by the Institutional Review Board of USC.

FD-OCT and Data Processing

The data acquisition was described previously.[5] Briefly, the eyes of study participants were scanned using the RTVue FD-OCT system (Optovue, Inc., Fremont, CA) using GCC and ONH scan patterns. The macular GCC scan protocol consisted of 14,928 A-scans over a 7-mm square area by using one horizontal line and 15 vertical lines at 0.5-mm intervals. The scans were centered 0.75 mm temporal to the fovea to improve the coverage of the temporal macula. Each eye was scanned three times and the images were checked for motion artifacts. The scans were exported and analyzed using proprietary software (written by Ou Tan) to remove outliers and filter the data. Segmentation was performed automatically. The GCC thickness was defined as the distance between the internal limiting membrane and the outer edge of the inner plexiform layer. The GCC map of 933 × 933 pixels was transformed into a 100 × 100 grid of "superpixels" to improve the speed of calculating correlations between maps. Each pixel was converted to a percent loss value, ranging from 0% to 100%, according to the equation % loss = 100*(normal − value)/normal. The GCC is too thin to be reliably measured by automated segmentation in and around the fovea and outside the macula. Therefore, the GCC thickness values within 0.75 mm of the foveal center and beyond 3 mm from the center of the scan were discarded. To simplify display and analysis, all NFL, GCC, and VF maps from left eyes were mirror-flipped to right-eye view. The ONH scan protocol uses a combination of radial and circular scans centered on the ONH. The circular scans around the ONH were used to measure NFL thickness profiles, which were in turn interpolated into an NFL map.

Pointwise Correlation Between GCC Thickness and NFL Thickness

The Pearson product-moment correlation coefficient (R) was calculated between GCC percent loss at every position within the 100 × 100 GCC superpixel map and each of 360° of the peripapillary NFL, which was also expressed as percent loss compared to normal. Each degree of the NFL was represented by the mathematical mean of the pixels within a wedge

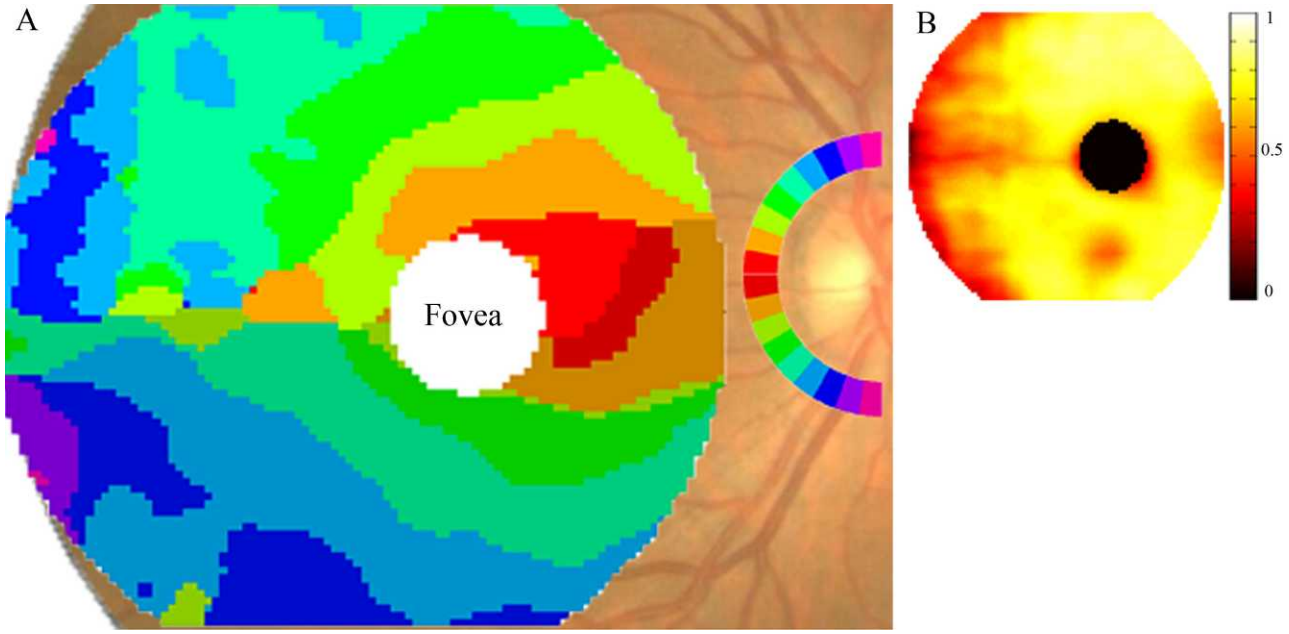

FIGURE 2. Map of correspondence between macular GCC loss and peripapillary NFL loss. (**A**) GCC map colored according to the highest correlating 10° angular sector of the peripapillary NFL. The inferior half of the peripapillary NFL is colored symmetrically to the superior half, but darker to allow differentiation between the two. (**B**) Pearson correlation coefficient R-value (ranges from 0 to 1) at each corresponding position of the GCC map in (**A**). The values range from 0.3 to 0.87.

extending 1° on either side of the degree being evaluated and radially 0.2 mm centered on a circle with diameter 3.4 mm.

Pointwise Correlation Between GCC Thickness and VF Defects

The Pearson product-moment correlation coefficient (*R*) was calculated between every position within the 100 × 100 GCC superpixel map, expressed as percent loss, and each of 52 positions within the 24-2 VF. The VF total deviation (TD) values at each position were entered manually point by point. They were then converted to percent loss (ranging from 0% to 100%) using the equation % loss = 100*(1 − $10^{[x/10]}$), where x is the decibel (dB) value of VF TD.

Regional Correlation Among GCC Thickness, NFL Thickness, and VF Defects

The GCC scan region was divided into four zones (superior versus inferior, and perifoveal versus macular), based on the optical area subserved by the VF divisions defined by Garway-Heath et al.[21] The theoretical border between the perifoveal

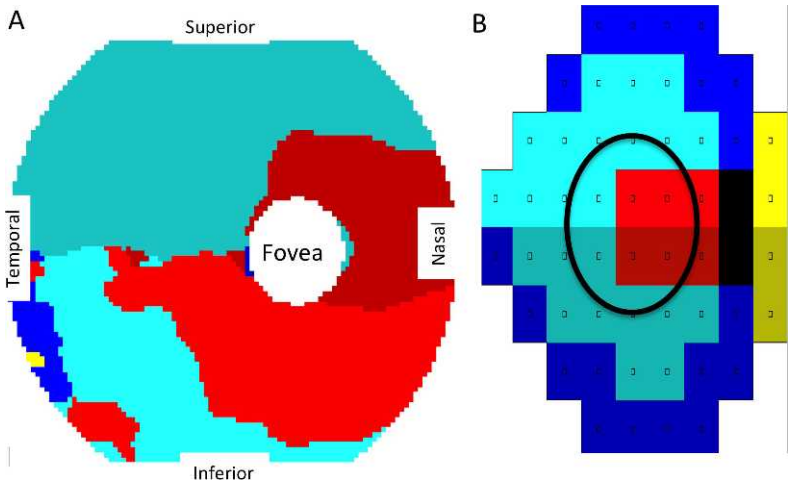

FIGURE 3. Map of correspondence between macular GCC loss and VF deficit. (**A**) The GCC map colored according to the highest correlating position in the Humphrey 24-2 VF shown in (**B**). (**B**) Humphrey 24-2 VF grouped according to the work of Garway-Heath et al.[21] The area circled in the VF roughly corresponds to the macular GCC scan area.

Investigative Ophthalmology & Visual Science

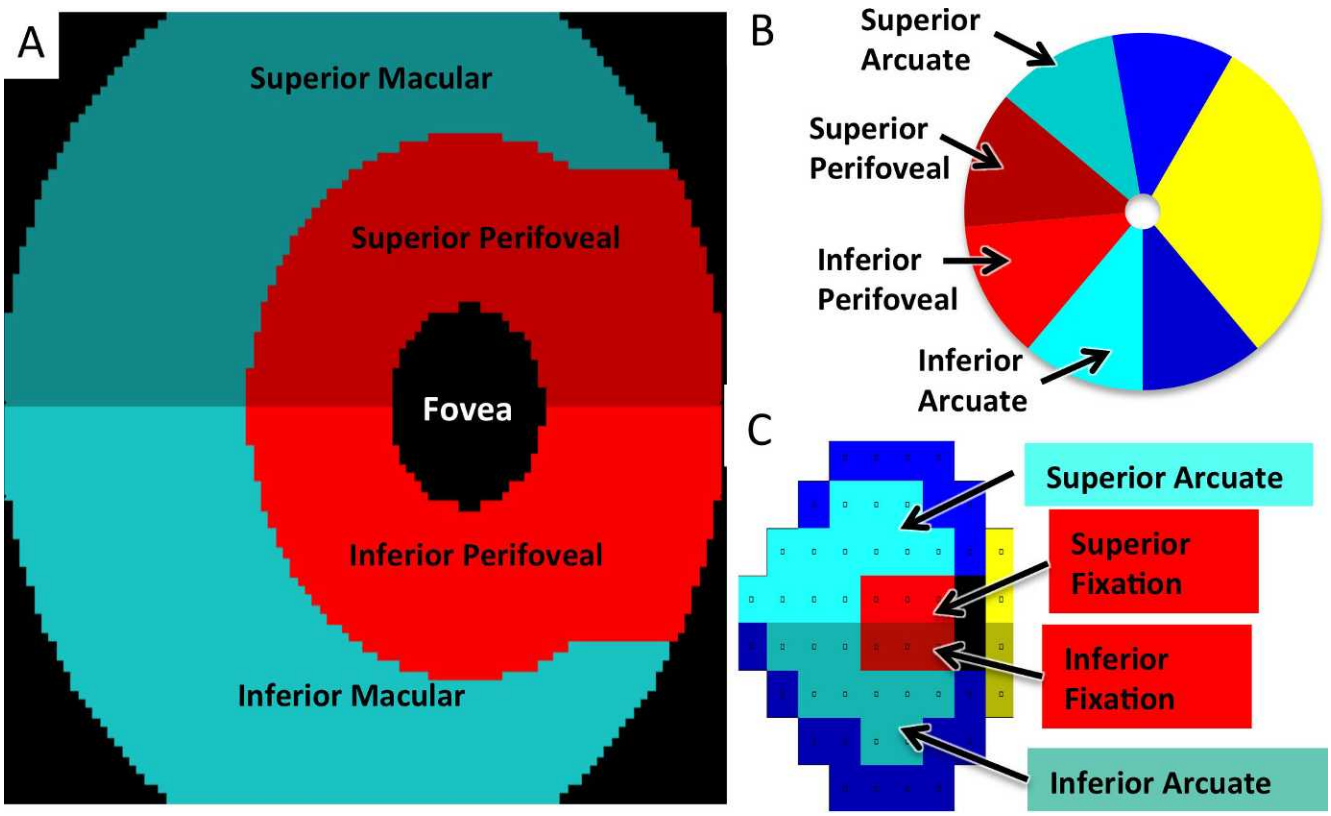

FIGURE 4. Macular GCC, VF, and NFL regions for correlation analysis. (**A**) The GCC map divided into superior and inferior perifoveal and macular regions for correlation analysis, taking parafoveal ganglion cell displacement into account. Colors represent anatomically related regions. (**B**) Peripapillary NFL divided into superior and inferior perifoveal and arcuate regions. The superior arcuate region extends from 100° to 140°. The superior perifoveal region extends from 140° to 185°. The inferior perifoveal region extends from 185° to 230°, and the inferior arcuate region extends from 230° to 270°. (**C**) Humphrey 24-2 VF divided into superior and inferior fixation and arcuate regions.

and macular GCC zones was determined by imposing a 6° VF grid over the retina, and then correcting for retinal ganglion cell displacement as previously described,[18,22] assuming that the vertical displacement was 76% of the horizontal displacement. This resulted in an ellipse with a horizontal (major) axis radius of 2.1175 mm and a vertical (minor) axis radius of 2.048 mm. Nasal to the ellipse we assumed that the vertical displacement was minimal and therefore used 6° vertically from the horizontal raphe as the border. We used the relationship 1 mm = arctan(1/17) degrees, according to the simple Gullstrand model.[23] The peripapillary NFL was similarly divided based on the work of Garway-Heath et al.[21] The perifoveal NFL extends from 40° above the horizontal to 50° below the horizontal. We chose 5° below the horizontal at the ONH as the border between the superior and inferior perifoveal regions, giving each region 45° in width. The mean percent loss for each VF region was calculated as the mean of the percent loss of all points within the VF region.

We used one randomly selected eye from each subject. We used least squares linear regression to calculate the regression line and slope, forcing the regression line to pass through the origin.

RESULTS

A total of 56 eyes from 38 subjects with perimetric glaucoma were included in the analysis. The mean age of the subjects was 64.5 years, and the average of the mean deviation (MD) for all visual fields was −4.4 dB (34 eyes with MD better than −6 dB, 18 eyes with MD between −12 dB and −6 dB, and 4 eyes with MD worse than −12 dB). An example of the complete dataset for an individual subject is shown in Figure 1.

The relationship between the two structural parameters, GCC loss and NFL loss, was analyzed. A correspondence map (Fig. 2) was constructed based on the assumption that anatomically connected areas of macular GCC and peripapillary NFL would have the highest correlation in glaucomatous loss. For each superpixel on the GCC map, we determined the most highly correlated angular sector (wedge) in the peripapillary NFL map (Fig. 2A). In the GCC area between the fovea and the ONH, the symmetry line is not horizontal, but is tilted along the fovea-ONH axis. Superior and inferior to the fovea, there are successive arcuate GCC areas that feed into the temporosuperior and temporoinferior NFL sectors. Again, superior-inferior symmetry is not strictly obeyed, there are inferior displacements of the corresponding NFL sectors. Temporal to the fovea, the superior and inferior halves of the GCC correspondence map are divided along the horizontal midline. But again the corresponding superotemporal and inferotemporal NFL sectors are inferiorly shifted. Another asymmetry is that the inferotemporal NFL sectors appear to correspond to larger patches of GCC, compared with superotemporal NFL sectors. The NFL sectors at the superior and inferior poles correspond to the temporal periphery of the GCC map, the arcuate connections being outside the GCC scan region and therefore not visible on the GCC map. The *R* values for the corresponding GCC and NFL areas ranged from 0.3 to 0.87 (Fig. 2B), with most of the perifoveal area having higher *R* values, whereas the lowest values occurred along the horizontal raphe and in the temporal periphery of the GCC

Investigative Ophthalmology & Visual Science

Table 1. Mean GCC and NFL Thickness in Normal Control Eyes

	GCC, μm	NFL, μm
Superior perifoveal	117.0	72.5
Superior macular/arcuate	79.5	116.2
Inferior perifoveal	116.5	68.2
Inferior macular/arcuate	80.0	126.4

Mean thickness for each GCC and NFL region shown in Figure 4 for 125 control eyes.

map. Overall, one observes that symmetric points above and below the horizontal midline in the GCC map correspond to locations on the peripapillary NFL that are not symmetric around the horizontal midline, but rather are shifted inferiorly at the ONH. Inferotemporal NFL sectors seem to serve larger areas of GCC compared with superotemporal NFL sectors at a similar distance above the horizontal midline. These features may be caused by the inferotemporal location of the fovea relative to the ONH.

We then determined for each GCC position the highest correlating VF position within the Humphrey 24-2 VF (Fig. 3). In this correspondence map, perifoveal GCC thinning correlates to VF defects near fixation, whereas GCC thinning in the peripheral macula correlates to more peripheral VF defects. There is a clear horizontal midline separating the superior and inferior zones within the correspondence map, confirmation of the optical projection relationship between GCC and VF. However, there is a slight asymmetry, the inferior GCC region corresponding to the superior fixation VF sector (bright red) is larger than the superior GCC region corresponding to the inferior fixation VF sector (dark red).

To divide the GCC map into regions based on visual function, we used previously published VF sectors[21] and performed optical projection onto the macula. After taking into account the centrifugal RGC displacement around the fovea,[22] this divided the GCC map into four regions: superior and inferior perifoveal versus peripheral macula (Figs. 4A–C). The peripapillary NFL was similarly divided into four regions, based on the work of Garway-Heath et al.[21] The theoretical division of the macular GCC map (Fig. 4A) resembles the one we obtained empirically (Fig. 3A), with the exception that the optical projection is symmetrical and does not account for the superior-inferior asymmetry in the perifoveal GCC zones seen in Figure 3.

A total of 125 eyes from 65 healthy control subjects were used to define the normal NFL and GCC thickness maps. This normative data is a snapshot of the baseline data from the longitudinal Advanced Imaging for Glaucoma Study and has been described in a previously published study on GCC.[5] The age was 52.9 ± 8.9 years (mean ± SD), and 68% were female. The mean GCC and NFL thickness for the four regions defined in Figure 4 are listed in Table 1. The perifoveal GCC regions are thicker than the peripheral macular GCC regions. The arcuate NFL regions are thicker than the perifoveal NFL regions, and the NFL is thicker in the inferior arcuate region compared with the superior arcuate region. The overall mean GCC thickness for the entire scan region in our control eyes was 94.7 μm.

For regional correlation analysis, GCC, NFL, and VF loss were all converted to units of percent loss relative to the normal values listed in Table 1. One eye from each of the 38 perimetric glaucoma subjects was randomly selected for the correlation analysis. This avoids the problem of artifactual increase in correlation coefficients due to correlation between the right and left eyes of the same individual. The same calculations were also performed using all 56 eyes with similar results (data not shown). First, the statistics for each GCC, NFL, and VF region were calculated (Table 2). The maximal GCC percent loss ranged from 42% to 49%, whereas the maximal NFL percent loss ranged from 66% to 84%. It is notable that the arcuate regions had greater loss compared with the fixation/perifoveal regions. The inferior fixation VF region was particularly well preserved compared with the degree of loss in the corresponding NFL and GCC regions.

The region with the greatest mean percent loss was the inferior macular GCC/inferior arcuate NFL/superior arcuate VF (Table 2, last row). The relationship between VF and GCC, as well as VF and NFL for this region was analyzed by linear regression (Figs. 5A, 5B). The intercepts at 100% VF loss are 47% GCC loss and 84% NFL loss. This would represent an estimate of end-stage residual thickness of 53% within the GCC and 16% within the NFL for this particular region. Linear regression analyses were also performed for other corresponding regions (plots not shown). The intercept analysis showed that at 100% VF loss, the estimated GCC loss would be 74%, 51%, and 50%, for the superior perifoveal, superior macular, and inferior perifoveal GCC regions, respectively. Similar intercept analysis for VF and NFL indicates that at 100% VF loss, the corresponding NFL loss would be 94%, 95%, and 68%, respectively. Averaged over the four regions, the mean end-stage loss was 56% for GCC and 85% for NFL, corresponding to residual thickness of 44% for GCC and 15% for NFL.

The regional correlation between the VF loss and GCC loss was examined (Table 3). For each VF region, the correlation was highest to the corresponding GCC region (entries along the diagonal). There was also significant correlation between adjacent GCC zones and VF regions, such as the "inferior-macular" GCC zone to the "superior-fixation" VF region.

We then analyzed the relationship between NFL loss and GCC loss (Table 4). As expected, the corresponding regions had the highest correlation coefficients (entries along the diagonal), with *R* values even higher than those found in Table 3. Again, we also found that anatomically adjacent regions were also significantly correlated.

Finally, we evaluated the correlation between VF loss and NFL loss (Table 5). Again, for each VF region, the matching NFL region had the highest correlation (entries along the diagonal).

Discussion

The development of commercial high-resolution FD-OCT opened the possibility of mapping inner retinal layers in the

Table 2. GCC, NFL, and VF Percent Loss per Region

GCC (NFL) Region	GCC Percent Loss, Mean ± SD, Maximum	NFL Percent Loss, Mean ± SD, Maximum	VF Percent Loss, Mean ± SD, Maximum	VF Region
Superior perifoveal	18.7 ± 14.0, 49.9	22.2 ± 19.7, 69.5	27.5 ± 27.5, 99.9	Inferior fixation
Superior macular, arcuate	19.2 ± 10.8, 41.5	35.3 ± 20.0, 74.0	37.8 ± 32.8, 99.9	Inferior arcuate
Inferior perifoveal	18.3 ± 12.1, 41.9	22.7 ± 8.6, 66.1	39.0 ± 33.2, 99.9	Superior fixation
Inferior macular, arcuate	21.6 ± 11.4, 42.6	39.4 ± 22.8, 84.1	47.7 ± 35.7, 99.9	Superior arcuate

The mean, SD, and maximum percent loss values are shown for each region.

Investigative Ophthalmology & Visual Science

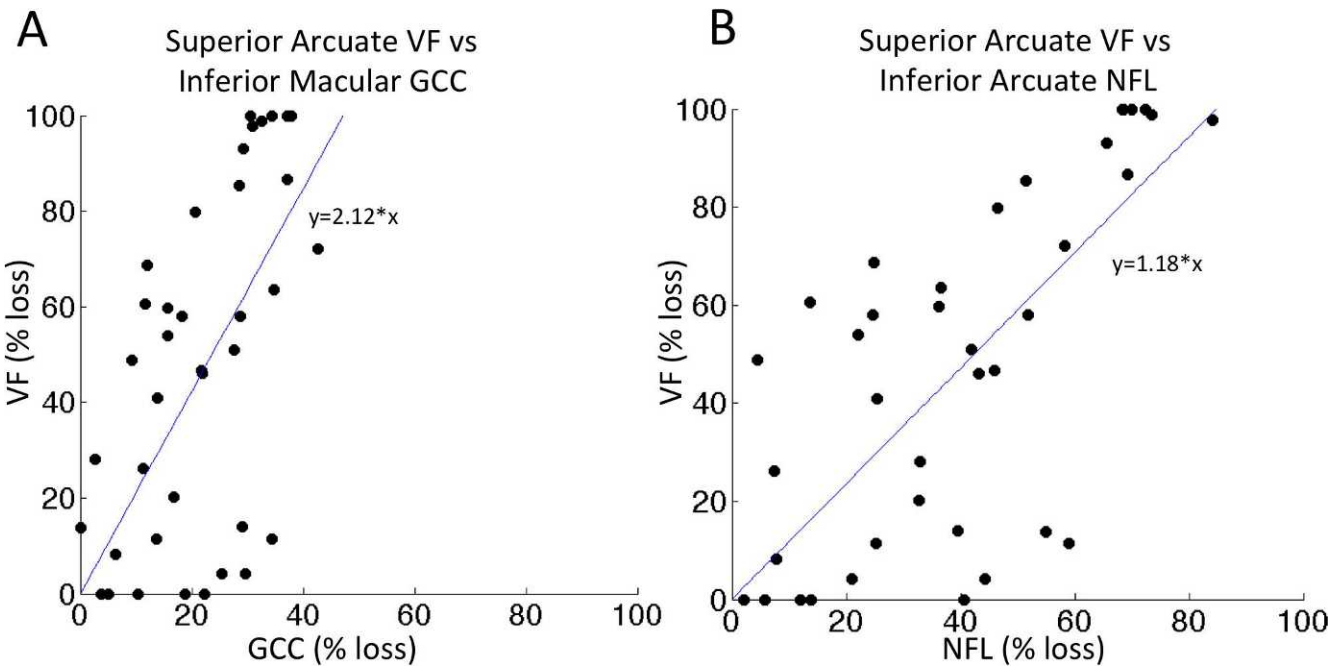

Figure 5. Scatterplot of VF versus GCC and VF versus NFL. Scatterplot and regression line for the region with the highest amount of damage in our dataset. (**A**) Superior arcuate VF versus inferior macular GCC; slope of the regression line Superior arcuate VF versus inferior arcuate NFL; slope of the regression line is 1.18. The regression lines were anchored at the origin.

retina for glaucoma assessment. The functional importance of the macula and central VF has motivated many recent studies in this area. Most of these studies have focused on the diagnostic power of global and hemifield macular GCC parameters. There were relatively few studies on the correlation between GCC and other anatomic and functional maps on a more spatially detailed basis. Our aim was to perform regional correlation between zones of the GCC map to zones of the NFL and VF maps. Understanding the regional correspondence will help clinicians interpret these structural maps in the context of VF defects. For instance, early glaucomatous changes on the VF may be differentiated from artifact by looking for loss on both the GCC and NFL maps in the corresponding zones.

The GCC-NFL correspondence map (Fig. 2) resembles a correlation map of the GCL+ (not GCC) to NFL recently published by Garvin and colleages.[16] Their macular region consisted of 66 squares, each 2° × 2° in size, which were correlated to 12 peripapillary NFL wedges, each 15° in size. The strength of their correlations (R^2 ranging from 0.24 in the fovea to 0.68 in the more peripheral areas of the scan) were similar to ours, although it is possible that some of their areas of low correlation were due to the inclusion of the horizontal raphe, which can be seen to have low R values on our map. Similar to our work, they also found that some areas of the macula had high correlation to multiple regions of the NFL. In subsequent work from the same group, Lee et al.[24] demonstrated that damage in ganglion-cell axonal complex, divided into 66 squares on a macular map, could be quantified and correlated with angular NFL sectors using automated image analysis of spectral-domain OCT images. We performed similar analysis at a higher resolution, using 10,000 points on the GCC map for correlation analysis. In addition, our correlation analyses included VF as well as NFL maps. Our higher spatial resolution helps us detect fine features, such as various forms of superior-inferior asymmetry. Of course, our high-resolution approach has a potential disadvantage: the resulting correspondence maps may contain more noise because noise filtering through spatial averaging was weaker.

Using the high-resolution GCC-NFL correlation map, we were able to detect superior-inferior asymmetry that is presumably the result of the ONH being superiorly positioned relative to the fovea. Some features of this asymmetry may partially explain the fact that glaucomatous damage is usually more severe and common in the inferior peripapillary NFL and the corresponding superior hemifield of vision. Hood and colleagues looked closely at RGC+ within the macula along with the 10-2 VF test, since it samples the central field better than the standard 24-2 VF.[18–20,25] Their observations showed that macular damage in glaucoma may be more common than previously realized, and that the inferior macula seemed more

Table 3. Correlation Between GCC and VF Regions

	VF Region			
GCC Zone	**Inferior Fixation**	**Inferior Arcuate**	**Superior Fixation**	**Superior Arcuate**
Superior perifoveal	**0.570 (0.0002)**	0.524 (0.0007)	0.192 (0.2491)	0.100 (0.5494)
Superior macular	0.405 (0.0117)	**0.611 (<0.0001)**	0.145 (0.3852)	0.044 (0.7935)
Inferior perifoveal	0.398 (0.0135)	0.248 (0.133)	**0.641 (<0.0001)**	0.418 (0.0090)
Inferior macular	0.238 (0.1495)	0.128 (0.4439)	0.601 (0.0001)	**0.585 (0.0001)**

The Pearson Product-Moment Correlation Coefficient R value (P value) was calculated between the mean percent loss within each GCC and VF region in Figure 4. The entries for corresponding regions are in bold.

Table 4. Correlation Between GCC and NFL Regions

	NFL Region			
GCC Zone	**Superior Perifoveal**	**Superior Arcuate**	**Inferior Perifoveal**	**Inferior Arcuate**
Superior perifoveal	**0.839 (<0.0001)**	0.661 (<0.0001)	0.659 (<0.0001)	0.272 (0.098)
Superior macular	0.774 (<0.0001)	**0.768 (<0.0001)**	0.584 (0.0001)	0.231 (0.1613)
Inferior perifoveal	0.618 (<0.0001)	0.442 (0.0055)	**0.871 (<0.0001)**	0.602 (0.0001)
Inferior macular	0.454 (0.0042)	0.335 (0.0398)	0.734 (<0.0001)	**0.746 (<0.0001)**

The Pearson Product-Moment Correlation Coefficient *R* (*P* value) was calculated between the mean percent loss within each GCC and NFL region in Figure 4. The entries for corresponding regions are in bold.

susceptible to damage than the superior macula. They hypothesized that superior retinal nerve fibers are less susceptible to glaucomatous damage because they enter the nerve head temporally, whereas the inferior fibers are more susceptible because they enter the more crowded inferotemporal area of the nerve, in what they term the "macular vulnerability zone."[19,20] Our results lend additional support to this crowding hypothesis. First, inferotemporal NFL sectors appeared to serve larger areas of the GCC than superotemporal NFL sectors at the same distance from the horizontal midline, and symmetric points about the fovea appeared to correspond to asymmetric locations on the ONH (Fig. 2). Second, in our control subjects, the NFL thickness in the "inferior arcuate" region was thicker than the "superior arcuate" region. Many published studies already showed that the inferior NFL quadrant is thicker than the superior quadrant,[26–28] but our results offer more direct evidence that the NFL sectors serving the inferior macular GCC region and the corresponding superior arcuate VF may indeed be more "crowded." These observations of asymmetry may offer only a partial explanation, however, as there are other possible asymmetries in vascular supply and ONH anatomy that may underlie glaucoma pathophysiology and are beyond the scope of the current study.

We also observed asymmetry between the superior and inferior perifoveal GCC regions relative to the VF (Fig. 3). This could be due to the asymmetric course of the NFL bundles. However, this asymmetry could also be due to the noise in our high-resolution GCC-VF correlation map. There is a limited range of glaucomatous loss patterns in our dataset, which contained only 56 eyes. These eyes had greater glaucomatous loss in the inferior perifoveal GCC (superior fixation VF region) than the superior perifoveal GCC (inferior fixation VF region) (VF 39% loss vs. 27.5% loss). The disease severity within the dataset affects the strength of the relationships that could be uncovered.[28] Thus the superior perifoveal region of our GCC correlation maps may be artifactually small due to the paucity of disease in this region. Su and colleagues[29] recently showed that initial parafoveal scotomas in glaucoma are more common and more severe superiorly. Other studies have also shown superior VF loss to be more common than inferior VF loss.[30,31] Another limitation of our study is that glaucomatous damage is usually contiguous in nature, often affecting adjacent areas of the retina and making our correlation maps less precise. Finally, the 24-2 VF used in our study is not the optimal SAP protocol to use to correlate the GCC and VF, as it does not sample the macula as well as a 10-2 VF.[18,19] However, the 24-2 is more commonly used in clinical practice, making our results more generalizable. Due to all of these limitations, we believe that correlations at the level of relatively broad regions as we have defined (Fig. 4) might be most practically useful at the current level of knowledge and OCT/VF technology.

The quantitative analysis of correlation (Tables 3–5) demonstrated significant correlation between corresponding regions of the GCC, NFL, and VF. Several other groups have recently published results examining the relationship between GCC, NFL, and VF data.[6,8,11,12] These studies have confirmed previously demonstrated correlation between NFL thickness and VF sensitivity,[32,33] while also showing significant correlation between GCC thickness and VF sensitivity. However, these studies have used much larger regions of the GCC, such as the entire superior or inferior half of the scan region, whereas in the present study we divided the GCC scan into four regions based on optical projection of previously published VF regions onto the macula. Our data also show significant correlation between some adjacent, noncorresponding regions, especially within the same superior or inferior hemifields. Other analyses have similarly encountered significant correlation between noncorresponding regions of the VF and NFL.[16,33] This likely represents the contiguous and often diffuse nature of glaucomatous damage, and a fundamental limitation to this type of approach.

The structural parameters, such as GCC and NFL thickness, are in units of microns on a linear scale, whereas the VF results are traditionally given in units of decibels on a logarithmic scale. Thus directly correlating structural (linear) and functional (dB) parameters results in a nonlinear relationship that can lead to the appearance of more structural loss early in the disease and more functional loss in late disease.[6,8,32,34] By converting both structural and functional measurements to units of percent loss, we found that they have a more linear relationship, although there is still relatively more severe VF damage in late disease (Fig. 5). Another approach to linearize VF data is to use the 1/Luminance (in lamberts) unit, which has

Table 5. Correlation Between NFL and VF Regions

	VF Region			
NFL Region	**Inferior Fixation**	**Inferior Arcuate**	**Superior Fixation**	**Superior Arcuate**
Superior perifoveal	**0.603 (0.0001)**	0.581 (0.0001)	0.222 (0.1805)	0.128 (0.4422)
Superior arcuate	0.469 (0.0030)	**0.610 (<0.0001)**	0.160 (0.3387	−0.037 (0.8262)
Inferior perifoveal	0.520 (0.0008	0.350 (0.0313)	**0.606 (0.0001)**	0.434 (0.0064)
Inferior arcuate	0.207 (0.2124)	0.025 (0.7898)	0.560 (0.0001)	**0.696 (<0.0001)**

The Pearson Product-Moment Correlation Coefficient *R* (*P* value) was calculated between the mean percent loss within each NFL and VF region in Figure 4. The entries for corresponding regions are in bold.

Investigative Ophthalmology & Visual Science

the advantage of having a simple physical meaning.[6,11,32] However, we prefer to use the percent loss unit because this allows us to look at the relationship between the structure and function at various disease stages. In particular, this allowed us to determine the residual GCC and NFL thickness for end-stage glaucoma (at or near 100% VF loss), representing glial tissue and blood vessels. Using the linear regression slope extrapolated to 100% VF loss, our estimate of end-stage residual thicknesses are 26% to 50% for GCC regions, and 6% to 32% for NFL regions. Using the maximal regional loss in our dataset (Table 2), our estimate of end-stage residual thicknesses are 50% to 58% for GCC regions, and 16% to 34% for NFL regions. In comparison, Aggarwal and colleagues[35] found average inferior and superior hemifield GCC residual thickness of 50.6 μm (53%) and 61.7 μm (64%), respectively, in subjects with nonarteritic ischemic optic neuropathy. Sihota et al.[36] reported an average residual NFL thickness of 44.9 μm (44%) in blind glaucoma eyes. Hood and colleagues[37] reported a residual NFL value of 45.5 μm (33%) in patients with ischemic optic neuropathy. Overall, our results gave estimates of residual GCC and NFL thicknesses that were slightly lower than previously published studies. Some of these differences may be due to the different OCT systems and image-processing software used. Notably, we also found that there may be superior-inferior asymmetries and arcuate-perifoveal differences in the end-stage residual thickness. These regional variations may have anatomic explanations that deserve further study.

Previous studies, including an early study by Sommer and colleagues,[1] to more recent studies,[34,38] suggest that it may be possible to reliably detect structural damage before being able to reliably detect VF loss on SAP. An important factor in determining whether this is possible is the variability associated with each test. The repeatability of global GCC measurements as measured by coefficient of variation (CV) ranges from 1.09% in healthy subjects[5] to 1.25% to 1.42% over a wide range of glaucoma subjects.[39] This can be more directly compared to SAP if the dB values are converted to percent loss. For instance, in healthy subjects, Brenton and Argus[40] measured short-term fluctuation at 1.3 dB (CV 4.3%), whereas Heijl et al.[41] similarly reported mean short-term fluctuation of 1.59 dB (CV 5.3%) peripherally and 1.25 dB (CV 4.2%) centrally. More studies are needed to directly compare the variability of VF, NFL, and GCC measurements at various stages of glaucoma severity.

There are many areas for future work. With a much larger dataset, it may be possible to make more accurate correlation maps. Another improvement would be the ability to scan larger regions of the posterior pole with newer models of FD-OCT that have higher scan speed. Other areas of research would include the ability to detect change or progression by analyzing scans of the same eye over time. More complex modeling can be applied to the relationship between structure and function, possibly even allowing us to predict function from structure as explored by Leite et al.,[27] Zhu et al.,[42] and Zhang et al.[17] In addition, using the regional relationship between GCC, NFL, and VF may improve the results of indices for staging and detecting glaucomatous damage that currently use global parameters, such as the combined index of structure and function (CSFI) described by Medeiros et al.[43]

In summary, we have established patterns of spatial correlation among GCC, NFL, and VF maps at both high- and low-resolution levels. We divided the GCC map into four regions that are suitable for clinical correlation with established NFL and VF sectors. Because an abnormal result on one test may be an artifact of segmentation or centration (OCT), or patient cooperation (VF), the presence of abnormalities in the corresponding regions of the other two tests indicates a true defect. Combining information from OCT and VF maps may enhance the ability to detect and confirm patterns of damage in the management of glaucoma patients.

Acknowledgments

Supported by National Institutes of Health Grants R01 EY013516 and P30 EY03040 and by a grant from Research to Prevent Blindness.

David Huang and Ou Tan have a significant financial interest in Carl Zeiss Meditec. Oregon Health and Science University (OHSU), David Huang, and Ou Tan have a significant financial interest in Optovue, a company that may have a commercial interest in the results of this research and technology. These potential conflicts of interest have been reviewed and managed by OHSU. Other authors have no commercial interest in any materials discussed in this article.

Disclosure: **P.V. Le**, None; **O. Tan**, Carl Zeiss Meditec (F), Optovue, Inc. (F), P; **V. Chopra**, None; **B.A. Francis**, None; **O. Ragab**, None; **R. Varma**, None; **D. Huang**, Carl Zeiss Meditec (F), Optovue, Inc. (F, I, C, R), P

References

1. Sommer A, Katz J, Quigley HA, et al. Clinically detectable nerve fiber atrophy precedes the onset of glaucomatous field loss. *Arch Ophthalmol*. 1991;109:77–83.
2. Townsend KA, Wollstein G, Schuman JS. Imaging of the retinal nerve fibre layer for glaucoma. *Br J Ophthalmol*. 2009;93:139–143.
3. Lin SC, Singh K, Jampel HD, et al. Optic nerve head and retinal nerve fiber layer analysis: a report by the American Academy of Ophthalmology. *Ophthalmology*. 2007;114:1937–1949.
4. Vizzeri G, Kjaergaard SM, Rao HL, Zangwill LM. Role of imaging in glaucoma diagnosis and follow-up. *Indian J Ophthalmol*. 2011;59:S59–S68.
5. Tan O, Chopra V, Lu AT, et al. Detection of macular ganglion cell loss in glaucoma by Fourier-domain optical coherence tomography. *Ophthalmology*. 2009;116:2305–2314.e1–2.
6. Cho JW, Sung KR, Lee S, et al. Relationship between visual field sensitivity and macular ganglion cell complex thickness as measured by spectral-domain optical coherence tomography. *Invest Ophthalmol Vis Sci*. 2010;51:6401–6407.
7. Kim NR, Hong S, Kim JH, Rho SS, Seong GJ, Kim CY. Comparison of macular ganglion cell complex thickness by Fourier-domain OCT in normal tension glaucoma and primary open-angle glaucoma. *J Glaucoma*. 2013;22:133–139.
8. Kim NR, Lee ES, Seong GJ, Kim JH, An HG, Kim CY. Structure-function relationship and diagnostic value of macular ganglion cell complex measurement using Fourier-domain OCT in glaucoma. *Invest Ophthalmol Vis Sci*. 2010;51:4646–4651.
9. Rolle T, Briamonte C, Curto D, Grignolo FM. Ganglion cell complex and retinal nerve fiber layer measured by fourier-domain optical coherence tomography for early detection of structural damage in patients with preperimetric glaucoma. *Clin Ophthalmol*. 2011;5:961–969.
10. Seong M, Sung KR, Choi EH, et al. Macular and peripapillary retinal nerve fiber layer measurements by spectral domain optical coherence tomography in normal-tension glaucoma. *Invest Ophthalmol Vis Sci*. 2010;51:1446–1452.
11. Rao HL, Zangwill LM, Weinreb RN, Sample PA, Alencar LM, Medeiros FA. Comparison of different spectral domain optical coherence tomography scanning areas for glaucoma diagnosis. *Ophthalmology*. 2010;117:1692–1699, 1699.e1.
12. Na JH, Kook MS, Lee Y, Baek S. Structure-function relationship of the macular visual field sensitivity and the ganglion cell complex thickness in glaucoma. *Invest Ophthalmol Vis Sci*. 2012;53:5044–5051.

13. Huang JY, Pekmezci M, Mesiwala N, Kao A, Lin S. Diagnostic power of optic disc morphology, peripapillary retinal nerve fiber layer thickness, and macular inner retinal layer thickness in glaucoma diagnosis with fourier-domain optical coherence tomography. *J Glaucoma*. 2011;20:87–94.
14. Rao HL, Babu JG, Addepalli UK, Senthil S, Garudadri CS. Retinal nerve fiber layer and macular inner retina measurements by spectral domain optical coherence tomograph in Indian eyes with early glaucoma. *Eye (Lond)*. 2012;26:133–139.
15. Mwanza JC, Durbin MK, Budenz DL, et al. Glaucoma diagnostic accuracy of ganglion cell-inner plexiform layer thickness: comparison with nerve fiber layer and optic nerve head. *Ophthalmology*. 2012;119:1151–1158.
16. Garvin MK, Abramoff MD, Lee K, Niemeijer M, Sonka M, Kwon YH. 2-D pattern of nerve fiber bundles in glaucoma emerging from spectral-domain optical coherence tomography. *Invest Ophthalmol Vis Sci*. 2012;53:483–489.
17. Zhang X, Bregman CJ, Raza AS, De Moraes G, Hood DC. Deriving visual field loss based upon OCT of inner retinal thicknesses of the macula. *Biomed Opt Express*. 2011;2:1734–1742.
18. Hood DC, Raza AS. Method for comparing visual field defects to local RNFL and RGC damage seen on frequency domain OCT in patients with glaucoma. *Biomed Opt Express*. 2011;2:1097–1105.
19. Hood DC, Raza AS, de Moraes CG, Johnson CA, Liemann JM, Ritch R. The nature of macular damage in glaucoma as revealed by averaging optical coherence tomography data. *Trans Vis Sci Tech*. 2012;1:1–15.
20. Hood DC, Raza AS, de Moraes CG, Liebmann JM, Ritch R. Glaucomatous damage of the macula. *Prog Retin Eye Res*. 2013;32:1–21.
21. Garway-Heath DF, Poinoosawmy D, Fitzke FW, Hitchings RA. Mapping the visual field to the optic disc in normal tension glaucoma eyes. *Ophthalmology*. 2000;107:1809–1815.
22. Drasdo N, Millican CL, Katholi CR, Curcio CA. The length of Henle fibers in the human retina and a model of ganglion receptive field density in the visual field. *Vision Res*. 2007;47:2901–2911.
23. Miller KM, Albert DL, Asbell PA, et al. *Basic and Clinical Science Course (BCSC) Section 3: Clinical Optics*. Singapore: American Academy of Ophthalmology; 2008:105–108.
24. Lee K, Kwon YH, Garvin MK, Niemeijer M, Sonka M, Abramoff MD. Distribution of damage to the entire retinal ganglion cell pathway: quantified using spectral-domain optical coherence tomography analysis in patients with glaucoma. *Arch Ophthalmol*. 2012;130:1118–1126.
25. Wang M, Hood DC, Cho JS, et al. Measurement of local retinal ganglion cell layer thickness in patients with glaucoma using frequency-domain optical coherence tomography. *Arch Ophthalmol*. 2009;127:875–881.
26. Paunescu LA, Schuman JS, Price LL, et al. Reproducibility of nerve fiber thickness, macular thickness, and optic nerve head measurements using StratusOCT. *Invest Ophthalmol Vis Sci*. 2004;45:1716–1724.
27. Leite MT, Zangwill LM, Weinreb RN, Rao HL, Alencar LM, Medeiros FA. Structure-function relationships using the Cirrus spectral domain optical coherence tomograph and standard automated perimetry. *J Glaucoma*. 2012;21:49–54.
28. Leung CK, Chan WM, Yung WH, et al. Comparison of macular and peripapillary measurements for the detection of glaucoma: an optical coherence tomography study. *Ophthalmology*. 2005;112:391–400.
29. Su D, Park SC, Simonson JL, Liebmann JM, Ritch R. Progression pattern of initial parafoveal scotomas in glaucoma [published online ahead of print November 10, 2012]. *Ophthalmology*. doi: 10.1016/j.ophtha.2012.08.018.
30. Hood DC, Raza AS, de Moraes CG, et al. Initial arcuate defects within the central 10 degrees in glaucoma. *Invest Ophthalmol Vis Sci*. 2011;52:940–946.
31. Gazzard G, Foster PJ, Viswanathan AC, et al. The severity and spatial distribution of visual field defects in primary glaucoma: a comparison of primary open-angle glaucoma and primary angle-closure glaucoma. *Arch Ophthalmol*. 2002;120:1636–1643.
32. Leung CK, Chong KK, Chan WM, et al. Comparative study of retinal nerve fiber layer measurement by Stratus OCT and GDx VCC, II: structure/function regression analysis in glaucoma. *Invest Ophthalmol Vis Sci*. 2005;46:3702–3711.
33. Gardiner SK, Johnson CA, Cioffi GA. Evaluation of the structure-function relationship in glaucoma. *Invest Ophthalmol Vis Sci*. 2005;46:3712–3717.
34. Hood DC, Kardon RH. A framework for comparing structural and functional measures of glaucomatous damage. *Prog Retin Eye Res*. 2007;26:688–710.
35. Aggarwal D, Tan O, Huang D, Sadun AA. Patterns of ganglion cell complex and nerve fiber layer loss in nonarteritic ischemic optic neuropathy by Fourier-domain optical coherence tomography. *Invest Ophthalmol Vis Sci*. 2012;53:4539–4545.
36. Sihota R, Sony P, Gupta V, Dada T, Singh R. Diagnostic capability of optical coherence tomography in evaluating the degree of glaucomatous retinal nerve fiber damage. *Invest Ophthalmol Vis Sci*. 2006;47:2006–2010.
37. Hood DC, Anderson S, Rouleau J, et al. Retinal nerve fiber structure versus visual field function in patients with ischemic optic neuropathy. A test of a linear model. *Ophthalmology*. 2008;115:904–910.
38. Harwerth RS, Vilupuru AS, Rangaswamy NV, Smith EL III. The relationship between nerve fiber layer and perimetry measurements. *Invest Ophthalmol Vis Sci*. 2007;48:763–773.
39. Sung MS, Kang BW, Kim HG, Heo H, Park SW. Clinical validity of macular ganglion cell complex by spectral domain-optical coherence tomography in advanced glaucoma [published online ahead of print December 3, 2012]. *J Glaucoma*. doi: 10.1097/IJG.0b013e318279c932.
40. Brenton RS, Argus WA. Fluctuations on the Humphrey and Octopus perimeters. *Invest Ophthalmol Vis Sci*. 1987;28:767–771.
41. Heijl A, Lindgren G, Olsson J. Normal variability of static perimetric threshold values across the central visual field. *Arch Ophthalmol*. 1987;105:1544–1549.
42. Zhu H, Crabb DP, Schlottmann PG, et al. Predicting visual function from the measurements of retinal nerve fiber layer structure. *Invest Ophthalmol Vis Sci*. 2010;51:5657–5666.
43. Medeiros FA, Lisboa R, Weinreb RN, Girkin CA, Liebmann JM, Zangwill LM. A combined index of structure and function for staging glaucomatous damage. *Arch Ophthalmol*. 2012;130:E1–E10.

Investigative Ophthalmology & Visual Science